Available online at www.sciencedirect.com
SCIENCE DIRECT®
Journal of Organometallic Chemistry 689 (2004) 585–594
Journal of Organometallic Chemistry
www.elsevier.com/locate/jorganchem

Ligand properties of aromatic azines: C–H activation, metal induced disproportionation and catalytic C–C coupling reactions

Daniel Dönnecke, Joachim Wunderle, Wolfgang Imhof *

Institut für Anorganische und Analytische Chemie der Friedrich-Schiller-Universität Jena, August-Bebel-Str. 2, 07743 Jena, Germany

Received 18 July 2003; accepted 10 November 2003

Abstract

The reaction of aromatic azines with $Fe_2(CO)_9$ yields dinuclear iron carbonyl cluster compounds as the main products. The formation of these compounds may be rationalized by a C–H activation reaction at the aromatic substituent in *ortho* position with respect to the exocyclic C–N double bond followed by an intramolecular shift of the corresponding hydrogen atom toward the former imine carbon atom. The second imine function of the ligand does not react. Additional products arise from the metal induced disproportionation of the azine into a primary imine and a nitrile. So also one of the imine C–H bonds may be activated during the reaction. Depending on the aromatic substituent of the azine ligands iron carbonyl complexes of the disproportionation products are isolated and characterized by X-ray crystallography. C–C coupling reactions catalyzed by $Ru_3(CO)_{12}$ result in the formation of *ortho*-substituted azines. In addition, *ortho*-substituted nitriles are identified as side-products showing that the metal induced disproportionation reaction also takes place under catalytic conditions.

1. Introduction

It is well accepted that organometallic compounds may be regarded as model compounds for intermediates in catalytic processes. During the last years our research was focussed on the chemistry of aromatic imines both in terms of iron carbonyl complexes derived from stoichiometric reactions of $Fe_2(CO)_9$ with the corresponding imine and ruthenium catalyzed C–C bond formation reactions starting from the same imines as the substrates. It became evident from these investigations that the initial step of the catalytic reactions is a metal induced C–H activation reaction which is also observed in the formation of the dinuclear iron carbonyl compounds with the same regioselectivity [1]. Some of the imines may be reacted with CO and ethylene in a three-component reaction to yield chiral lactams [2].

In order to achieve a reaction with an enhanced atom economy we considered the use of azines as the substrates. Aromatic azines represent diimines with two potential reaction sites for the catalytic synthesis of heterocyclic compounds in which the unsaturated imine moieties are connected by a N–N bond.

The organometallic chemistry of azines has been the subject of quite a number of publications in the last decades. Most of the reactions lead to the symmetrical cleavage of the azine moiety producing two imide units which undergo subsequent reactions [3]. Very recently, the rhodium induced cleavage of an azine into a nitrile and a imine has been reported and the molecular structure of the corresponding nitrile complex was determined [4]. In context with our research on iron or ruthenium induced C–H activation reactions the reactivity of aromatic imines towards iron carbonyls was of considerable interest. It was reported that in analogy to other transition metals the reaction of ketazines with iron carbonyls leads to the formation of bis(μ-iminato) complexes by a symmetrical cleavage of the N–N bond of the corresponding azine [5]. Azines derived from aromatic aldehydes upon reaction with iron carbonyls yield dinuclear complexes in which one of the C–H bonds of the aromatic substituent is activated and the hydrogen atom is transferred towards the former imine carbon atom whereas the N–N bond is still preserved [6].

* Corresponding author. Tel.: +49-3641-948144; fax: +49-3641-948102.
E-mail address: cwi@rz.uni-jena.de (W. Imhof).

0022-328X/$ - see front matter © 2003 Elsevier B.V. All rights reserved.
doi:10.1016/j.jorganchem.2003.11.018

The same reaction sequence of C–H activation and hydrogen transfer is observed for aromatic imines in general and is believed to be closely related to the initial reactions during the catalytic C–C coupling induced by ruthenium precatalysts in the same position of the ligands [1,2]. In some reactions of azines with $Fe_3(CO)_{12}$ trinuclear compounds are formed in which the third iron carbonyl moiety is coordinated to the aromatic substituent in an η^6-fashion [7]. Treatment of acetaldazine with $Fe_3(CO)_{12}$ yields a dinuclear pyrazolidin-diyl ligand by an intramolecular ring closure following the activation of a C–H bond of one of the methyl groups [8]. In contrast the reaction of iron carbonyls with azine ligands derived from cinnamaldehyde yields mono- or dinuclear iron carbonyl complexes, in which 1-azadiene substructures of the ligand are η^4-coordinated to the metal atoms [9].

We report herein the reaction of a series of aromatic aldazines with $Fe_2(CO)_9$ yielding the expected dinuclear iron complexes as the main products. We were also able to isolate additional products generated by a non-symmetrical cleavage of the azines. Depending on the aromatic substituent iron carbonyl complexes of the nitrile or of the primary imine may be isolated. The latter are the first examples of imine complexes produced by the metal mediated cleavage of an azine. We will also report on catalytic C–C coupling reactions in the presence of $Ru_3(CO)_{12}$ as the precatalyst.

2. Results and discussion

2.1. Stoichiometric reactions with $Fe_2(CO)_9$

The azines **1**–**4** are easily obtained by the reaction of hydrazine hydrate with the corresponding aldehyde in ethanol. Scheme 1 shows the reaction of the azine ligands with $Fe_2(CO)_9$ to produce the iron carbonyl cluster compounds **5**–**7** and **9**–**13**, respectively. In all reactions we performed the dinuclear iron carbonyl compounds **5**, **6**, **9** or **12** were the main products, the reaction of the bis(β-naphthyl)-azine yields only the dinuclear complex **5**. The formation of these complexes proceeds via a C–H activation reaction at the aromatic substituent in *ortho* position with respect to the exocyclic imine moiety. The corresponding hydrogen atom is

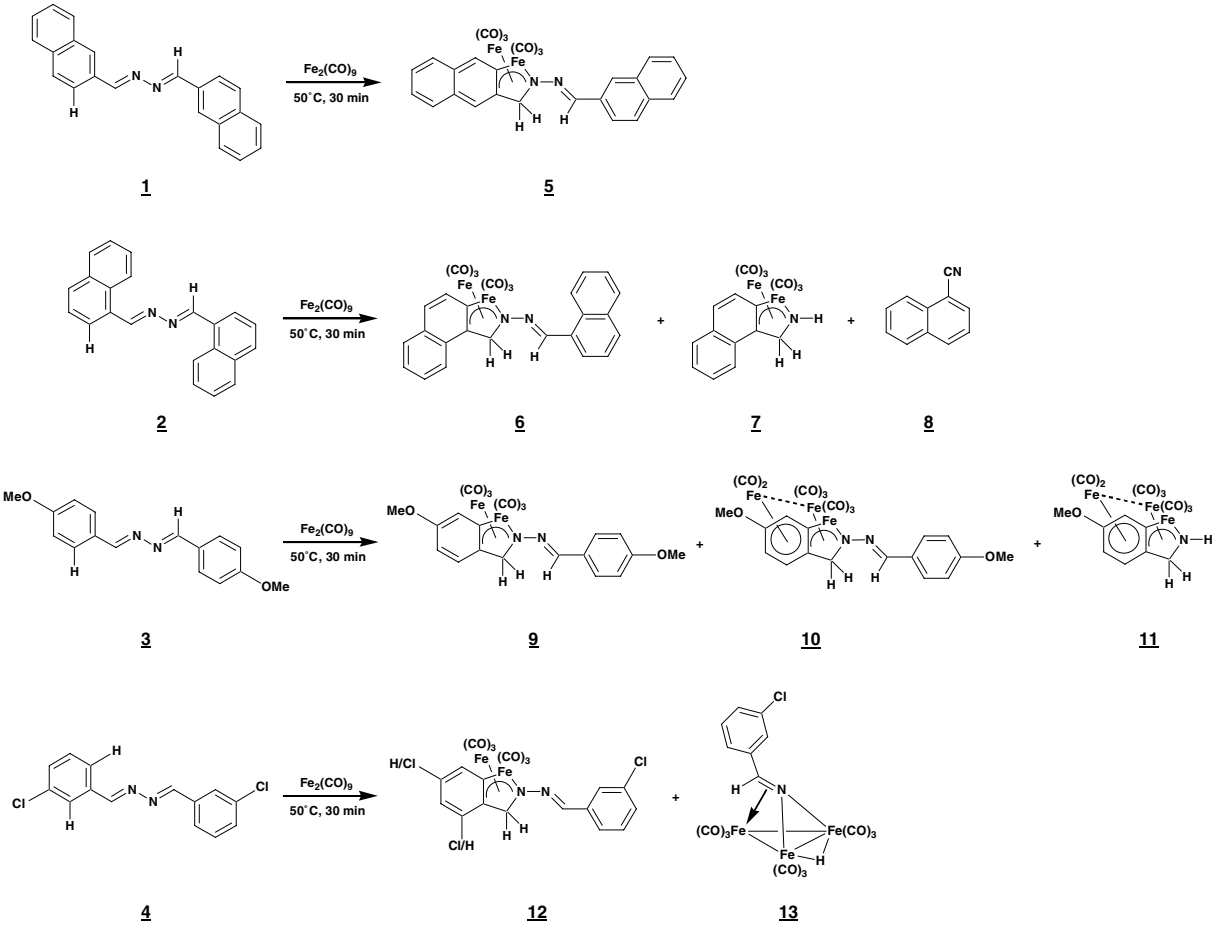

Scheme 1.

transferred towards the former imine carbon atom producing a methylene group. So the observation of a singlet at about 4 ppm in the ^{1}H NMR as well as a signal at about 70 ppm in the ^{13}C NMR clearly indicates the formation of **5**, **6**, **9** or **12**. It is remarkable that we never observed the formation of a compound in which both imine functions of the azine ligands reacted in that manner. So obviously the coordination of a $Fe_2(CO)_6$ moiety to the ligand system decreases the ability of the second imine moiety to interact with additional transition metal centers.

Fig. 1 shows the molecular structure of **6**, the most important bond lengths and angles are depicted in the figure caption. In accordance with the molecular structures of other iron carbonyl complexes of aromatic imines [1], one of the imine functions of the azine **2** is transformed into a formally 6e-donating enyl-amido ligand coordinating a $Fe_2(CO)_6$ moiety. Another description would be that of an aza-metalla-cyclopentadiene ligand with another apical $Fe(CO)_3$ group attached to it. The second imine moiety is not coordinated to iron carbonyl fragments and the naphthyl substituent is turned out of the plane of the aza-ferracyclopentadiene by 56.9°. The bond between N1 and N2 clearly represents a N–N single bond and is only slightly elongated compared to corresponding bonds in uncoordinated azines.

The molecular structure of **12**, which is presented in Fig. 2 together with the most important bond lengths and angles, is closely related to that of **6**. The coordination mode of the iron carbonyl fragments is nearly identical. The only difference is the bond between the apical $Fe(CO)_3$ group and C2, which is about 20 pm longer in **12** when compared with **6**. Since in the azine **4** the aromatic substituent exhibits a chlorine atom in *meta* position with respect to the imine function, in principle two different pathways of the C–H activation/hydrogen transfer reaction sequence are possible. In one of them the C–H bond *ortho* to both substituents at the aromatic system would be activated leading to the isomer of **12** as it is shown in Fig. 2. The other reaction pathway then would proceed via the activation of the C–H bond in trans position to the chlorine atom. Indeed both reaction pathways are observed by NMR spectroscopy in a 70:30 ratio preferring the formation of the isomer shown in Fig. 2. Interestingly, in the crystal structure of **12** both isomers are statistically disordered in the same ratio. Fig. 2 shows the isomer with the higher occupation factors.

The reaction of the azine derived from hydrazine and *p*-methoxybenzaldehyde produces the trinuclear compound **10** in small yields. The cluster is closely related to **9**, since the same C–H activation and hydrogen transfer reaction sequence has been performed ending up in the formation of an enyl-amido ligand. But in contrast to **9** three iron carbonyl moieties are coordinating the ligand. Two of them show the same coordination mode as it is observed for the dinuclear derivatives **5**, **6**, **9** and **12**. In addition, a third $Fe(CO)_2$ group is η^6-coordinated to the aromatic ring. Although we did not achieve crystals of

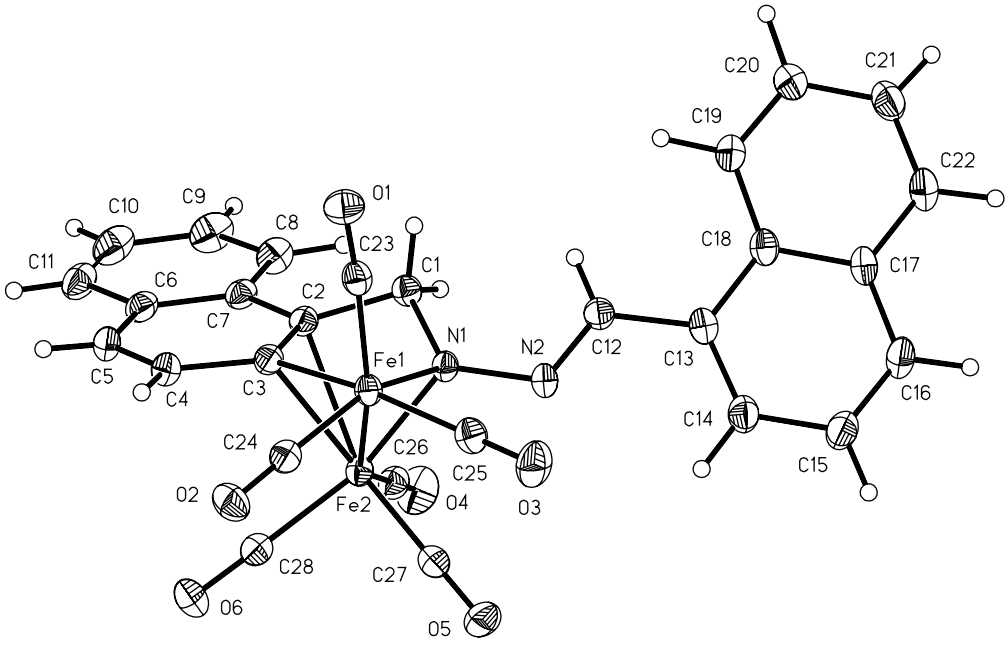

Fig. 1. Molecular structure of **6**; selected bond lengths (pm) and angles (°): Fe1–Fe2 243.68(4), Fe1–N1 197.3(2), N1–C1 147.1(2), C1–C2 150.8(3), C2–C3 140.9(3), Fe1–C3 198.0(2), Fe2–N1 196.4(2), Fe2–C2 227.4(2), Fe2–C3 217.2(2), N1–N2 140.7(2), N2–C12 128.5(2); N1–Fe1–C3 77.94(7), Fe1–C3–C2 114.6(1), C3–C2–C1 114.2(2), C2–C1–N1 99.5(1), C1–N1–Fe1 114.1(1), Fe1–N1–N2 120.6(1), C1–N1–N2 119.2(1), N1–N2–C12 118.0(2), N2–C12–C13 120.9(2).

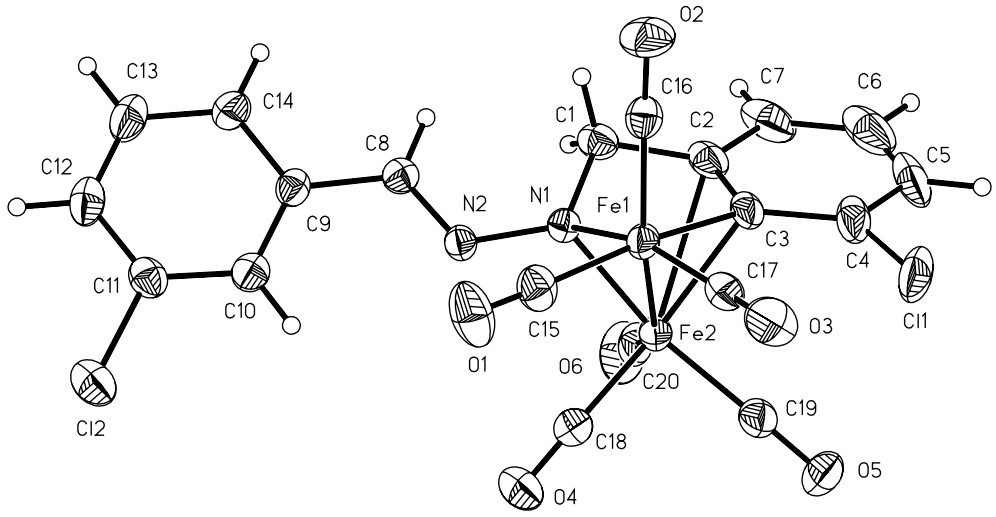

Fig. 2. Molecular structure of **12**; selected bond lengths (pm) and angles (°): Fe1–Fe2 243.43(6), Fe1–N1 196.5(2), N1–C1 147.5(4), C1–C2 150.1(5), C2–C3 141.3(5), Fe1–C3 200.2(3), Fe2–N1 195.4(2), Fe2–C2 247.4(3), Fe2–C3 218.4(3), N1–N2 141.5(3), N2–C8 127.4(4); N1–Fe1–C3 77.4(1), Fe1–C3–C2 112.8(2), C3–C2–C1 115.5(3), C2–C1–N1 100.9(3), C1–N1–Fe1 112.8(2), Fe1–N1–N2 115.9(2), C1–N1–N2 118.8(2), N1–N2–C8 118.4(2), N2–C8–C9 121.1(3).

sufficient quality to perform a X-ray structure determination, the structure of **10** is unequivocally demonstrated by its spectroscopic data [7].

The most interesting feature of the reaction of aromatic azines with $Fe_2(CO)_9$ is the observation of products that arise from the unsymmetrical formal disproportionation of the azine into an imine and a nitrile. To the best of our knowledge a reaction like this has not been reported from the treatment of azines with iron carbonyls. Very recently a closely related reaction was described starting from a rhodium pincer complex exhibiting the very labile dinitrogen ligand [4].

Depending on the aromatic substituent we were able to isolate either complexes formally derived from the primary imine (**7** and **11**) or from the nitrile (**13**). In one case the nitrile itself was detected by means of IR spectroscopy (**8**). The disproportionation of the azine ligands can only proceed via the activation of the imine C–H bond of the second imine moiety followed by the transfer of this hydrogen atom towards the former imine nitrogen atom together with a cleavage of the N–N bond of the azines. The question then arises whether the formation of **7**, **8**, **11** and **13** is just the result of a thermal decomposition of the dinuclear complexes **6**, **9** and **12**. Then the C–H activation of the imine hydrogen atom would be due to the electron deficiency of the α,β-unsaturated diimine system induced by the coordination of the $Fe_2(CO)_6$ moiety. Another possibility would be the coordination of additional iron carbonyl fragments to **6**, **9** and **12** leading to the observed unsymmetrical cleavage of the azines. To us the latter possibility seems to be more reasonable, since stirring a solution of **6** in heptane at 50 °C does not lead to the formation of **7**. On the other hand, the reaction of **6** with additional $Fe_2(CO)_9$ under the same reaction conditions produces **7**, although the yields are as low as in the reaction of $Fe_2(CO)_9$ with the free azine **2**.

The molecular structure of **7** is shown in Fig. 3 together with the most important bond lengths and angles in the figure caption. Formally **7** is a $Fe_2(CO)_6$ complex of a primary imine that also showed the reaction sequence of *ortho*-metallation and subsequent hydrogen transfer towards the imine carbon atom. The fact that in the related cleavage of an azine by a rhodium complex

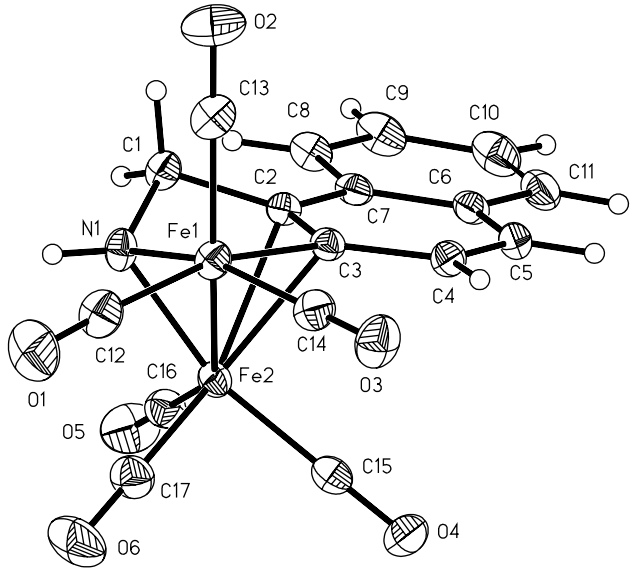

Fig. 3. Molecular structure of **7**; selected bond lengths (pm) and angles (°): Fe1–Fe2 245.75(3), Fe1–N1 194.4(1), N1–C1 146.5(2), C1–C2 150.9(2), C2–C3 141.6(2), Fe1–C3 198.9(2), Fe2–N1 194.8(2), Fe2–C2 228.9(2), Fe2–C3 217.4(2); N1–Fe1–C3 77.76(6), Fe1–C3–C2 114.2(1), C3–C2–C1 113.4(1), C2–C1–N1 99.6(1), C1–N1–Fe1 114.3(1).

no imine and no complex of the imine was detectable [4] to our opinion is an additional hint that in the reaction described herein the cleavage of the N–N bond of the azine follows the reaction of the first imine moiety of the ligand. The hydrogen atom at the former imine nitrogen atom gives rise to characteristic signals in the IR- and NMR-spectra of **7** (cf. Section 3). The coordination of the enyl-amido ligand in **7** is very similar as in **6** with the exception that the nitrogen atom is more basic in **7** because of the loss of the second imine moiety and thus the nitrogen iron bond lengths are decreased to some extend.

If the azine from *p*-methoxybenzaldehyde (**3**) is used in the reaction a very similar iron carbonyl complex of a primary imine may be isolated. The molecular structure of the trinuclear cluster **11** is depicted in Fig. 4. **11** also shows a hydrogen atom at the former imine nitrogen as well as a methylene group at the former imine carbon atom (C1). The C–H bond in *ortho* position with respect to the former imine substituent has been activated. The main difference in this compound compared to the molecular structures of **6**, **7** and **12** is the fact that the aromatic substituent is coordinated to a third iron carbonyl moiety in a η^6-fashion. Due to the coordination of a third iron carbonyl fragment the C2–Fe2 distance in **11** is extremely elongated. The iron–iron bond between Fe2 and Fe3 also seems to be quite labile. Compounds closely related to **11** were described earlier from the reaction of azines with $Fe_3(CO)_{12}$, although in these cases the N–N bond of the azines was preserved and the second imine function in analogy to the formation of **6**, **9** and **12** did not react [7]. The hydrogen atom at N1 again is clearly identified by IR spectroscopy.

Another trinuclear cluster compound was produced in the reaction of the azine **4** with $Fe_2(CO)_9$. The molecular structure of **13** is shown in Fig. 5 together with the most important bond lengths and angles. The cluster is best described as a Fe_3N-tetrahedron with the nitrogen atom still being part of an imine function. The carbon nitrogen bond represents a double bond which is slightly elongated due to the side-on coordination of this imine double bond to one of the iron atoms. The iron–iron bond between the other two iron centers is bridged by a hydrido ligand. Although there is an imine hydrogen atom present in the molecular structure of **13**, we still think that this compound is derived from the nitrile which is produced by the unsymmetrical cleavage of the azine **4**. The best evidence for this assumption is the fact, that the only time that compounds of analogous composition were synthesized, nitriles and carbonyl ferrates were reacted in the presence of a proton source [10].

2.2. Catalytic alkylation of the naphthylazines *1* and *2*

Aromatic imines may be reacted with CO and/or alkenes in the presence of catalytic amounts of

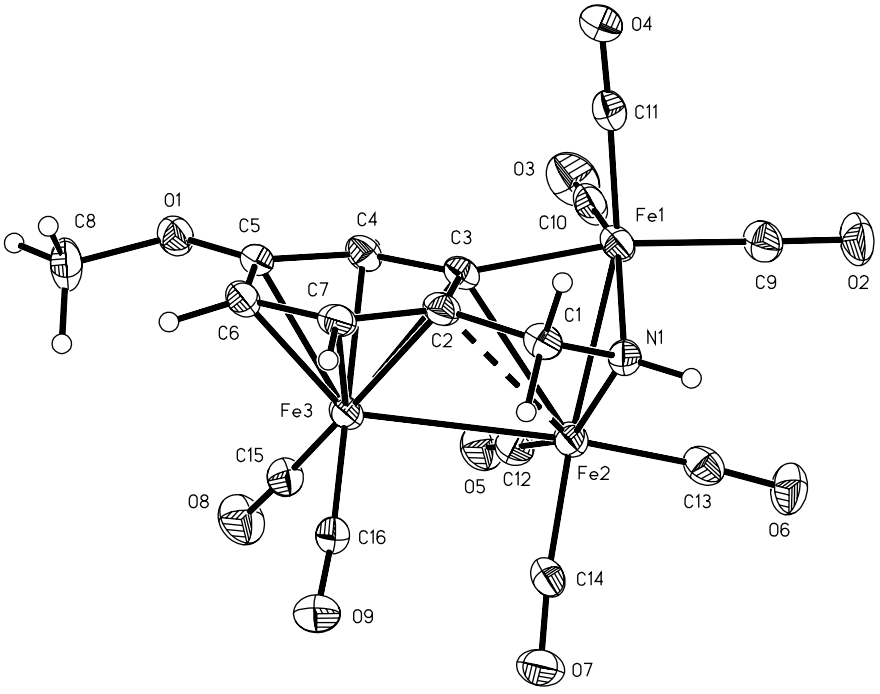

Fig. 4. Molecular structure of **11**; selected bond lengths (pm) and angles (°): Fe1–Fe2 246.6(1), Fe2–Fe3 283.8(1), Fe1–N1 197.4(5), N1–C1 147.2(7), C1–C2 148.7(7), C2–C3 143.9(7), Fe1–C3 197.5(5), Fe2–N1 196.9(4), Fe2–C2 294.0(9), Fe2–C3 249.6(5); Fe3–C2 212.3(5), Fe3–C3 221.4(5), Fe3–C4 213.5(5), Fe3–C5 218.3(5), Fe3–C6 213.2(6), Fe3–C7 211.4(5), Fe1–Fe2–Fe3 95.4(4), N1–Fe1–C3 77.1(2), Fe1–C3–C2 113.6(4), C3–C2–C1 113.6(5), C2–C1–N1 104.2(4), C1–N1–Fe1 112.7(4).

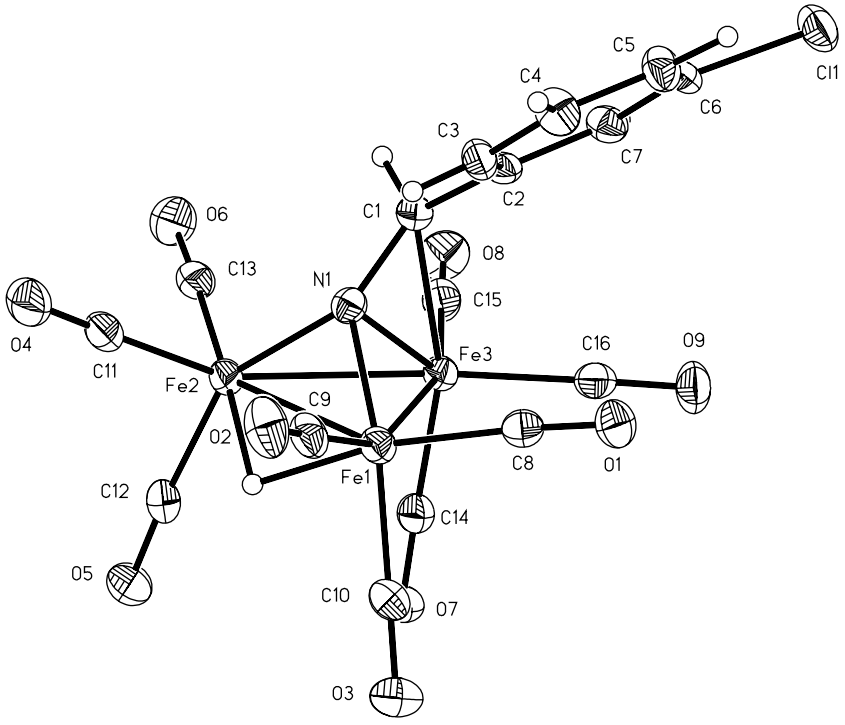

Fig. 5. Molecular structure of **13**; selected bond lengths (pm) and angles (°): Fe1–Fe2 258.5(1), Fe1–Fe3 254.9(1), Fe2–Fe3 255.7(1), Fe1–N1 186.6(5), Fe2–N1 185.8(4), Fe3–N1 194.8(4), Fe3–C1 220.4(6), N1–C1 134.7(7), C1–C2 148.2(7); Fe1–Fe2–Fe3 59.44(3), Fe2–Fe3–Fe1 60.81(3), Fe3–Fe1–Fe2 59.75(3), Fe1–N1–Fe2 87.9(2), N1–Fe2–Fe1 46.2(2), Fe2–Fe1–N1 45.9(1), Fe1–N1–Fe3 83.9(2), N1–Fe3–Fe1 46.7(1), Fe3–Fe1–N1 49.4(1), Fe2–N1–Fe3 84.4(2), N1–Fe3–Fe2 46.3(1), Fe3–Fe2–N1 49.3(1), Fe3–N1–C1 81.8(3), N1–C1–Fe3 61.0(3), C1–Fe3–N1 37.2(2), Fe3–C1–C2 121.9(4), N1–C1–C2 122.6(5).

$Ru_3(CO)_{12}$ to produce compounds, in which the co-substrates are formally inserted into the C–H bond in *ortho* position with respect to the imine function [11]. So presumably the imine substituent acts as a donor site for the catalytically active organometallic species thus controlling the regioselectivity of the C–H activation reaction. This step of the catalytic reaction is then closely related to the stoichiometric C–H activation reactions described above. The reaction of α-naphthylimines with ethylene yielded naphthaline derivatives with an ethyl group in 2-position. On the other hand, the reaction of β-naphthylimines with CO and ethylene ended up in the formation of heterocyclic products [2b].

Scheme 2 shows the products we observed from the catalytic reaction of **2** with ethylene in the presence of $Ru_3(CO)_{12}$. GC- and GC-MS measurements showed that the starting compound has been fully consumed after 16 h and that the main product is the doubly alkylated species **14**. The formation of this compound corresponds to the C–H activation reactions described above, in which the central C–C bond of the azine substrate is not cleaved. Most remarkably, we also observed the formation of **15** in a 10% yield. The identity of **15** is unequivocally shown by comparison of its spectra with those reported in the literature [12]. So the second reactivity pattern in the stoichiometric reactions – the metal induced dispropor-

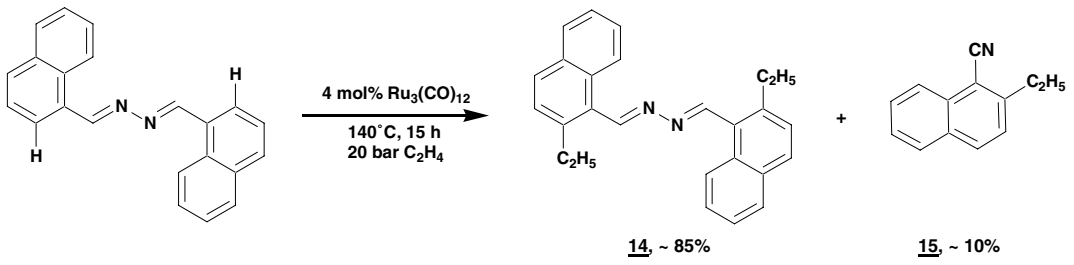

Scheme 2.

tionation of the azine ligands – is also a model for the formation of the side-product of the catalytic reactions.

3. Experimental

3.1. General

All procedures were carried out under an argon atmosphere in anhydrous, freshly distilled solvents.

Infrared spectra were recorded on a Perkin–Elmer FT-IR System 2000 using 0.2 mm KBr cuvettes. NMR spectra were recorded on a Bruker AC 200 spectrometer (^{1}H: 200 MHz, ^{13}C: 50.32 MHz, $CDCl_3$ as internal standard). Mass spectra were recorded on a Finnigan MAT SSQ 710 instrument. Elemental analyses were carried out at the Institute of Organic and Macromolecular Chemistry at the Friedrich-Schiller-University Jena using a LECO-CHNS-932 system.

3.2. X-ray crystallographic studies

The structure determinations of **6**, **7**, **11**, **12** and **13** were carried out on an Enraf Nonius Kappa CCD diffractometer, crystal detector distance 25 mm, using graphite monochromated Mo Kα radiation. The crystal was mounted in a stream of cold nitrogen. Data were corrected for Lorentz and polarization effects but not for absorption. The structure was solved by direct methods and refined by full-matrix least-squares techniques against F^2 using the programs SHELXS-86 and SHELXL-93 [13]. Computation of the structure was accomplished with the program XPMA [14] and the molecular illustration was drawn using the program XP [15]. The crystal and intensity data are given in Table 1.

3.3. Synthesis of 5–13

A 182 mg portion $Fe_2(CO)_9$ (0.5 mmol) together with an equimolar amount of the corresponding azine (154 mg **1**, 154 mg **2**, 134 mg **3**, 138 mg **4**) and 20 ml *n*-heptane are stirred together at 50 °C for 30 min. In the course of the reaction the pale yellow suspension slowly changes to a deep red solution as the ligand and $Fe_2(CO)_9$ dissolve. After the reaction is completed all volatile materials are removed in vacuo. The residue is dissolved in CH_2Cl_2, 1 g silanized silica gel is added and the solvent is again removed under reduced pressure. Chromatography on silica gel using light petroleum (b.p. 40–60 °C) as the eluent first yields a small green band containing $Fe_3(CO)_{12}$. Adding small portions of CH_2Cl_2 to the light petroleum allows the elution of the iron carbonyl compounds **5**–**7** and **9**–**13**. In each reaction the complexes resulting from a cleavage of the N–N bond of the azines (**7**, **11** and **13**) elute prior to the main products (**5**, **6**, **9** and **12**). Chromatography of the product mixture from the reaction of the methoxy-substituted azine **3** yields a fraction containing **9** and **10**, which can be separated repeating the chromatography using mixtures of light petroleum (b.p. 40–60 °C) and toluene. In addition, using pure CH_2Cl_2 or diethylether as the solvent results in the elution of approximately 0.25 mmol of the corresponding azine. The formation of **8** was confirmed by its IR spectrum. Yields (based on the portion of the converted azines): 35 mg **5** (0.06 mmol, 24%), 38 mg **6** (0.06 mmol, 26%), 4 mg **7** (0.01 mmol, 4%), 38 mg **9**, (0.07 mmol, 28%), 10 mg **10** (0.02 mmol, 6%), 2 mg **11** (0.004 mmol, 2%), 17 mg **12** (0.03 mmol, 12%), 2 mg **13** (0.004 mmol, 1%). Due to the very low yields of **7**, **10**, **11**, and **13** elemental analyses and NMR spectra could not be obtained for all compounds. Nevertheless, the molecular structure of these complexes was unequivocally demonstrated by X-ray analyses (**7**, **11** and **13**) or by comparison of the spectroscopic properties with those of closely related compounds reported in the literature (**10**) [7]. Recrystallization of the complexes was performed from mixtures of light petroleum (b.p. 40–60 °C) and CH_2Cl_2 at −20 °C.

3.4. MS and spectroscopical data for 5

Anal. Calc. for $C_{28}H_{16}N_2O_6Fe_2$: C, 57.18; H, 2.74; N, 4.76. Found: C, 56.58; H, 2.92; N, 4.21%. DEI *m*/*z* (%): 588 (M^+, 4), 560 (M^+–CO, 18), 532 (M^+–2CO, 18), 504 (M^+–3CO, 17), 476 (M^+–4CO, 19), 448 (M^+–5CO, 11), 420 (M^+–6CO, 74), 392 (M^+–$Fe_2(CO)_3$, 2), 364 (M^+–$Fe_2(CO)_4$, 3), 336 (M^+–$Fe_2(CO)_5$, 2), 308 (M^+–$Fe_2(CO)_6$, 19), 280 ($Fe_2(CO)_6^+$, 9), 252 ($Fe_2(CO)_5^+$, 3) 224 ($Fe_2(CO)_4^+$, 8), 196 ($Fe(CO)_5^+$, 30), 168 ($Fe(CO)_4^+$, 30), 153 ($C_{11}H_7N^+$, 61), 140 ($Fe(CO)_3^+$, 17), 112 ($Fe(CO)_2^+$, 28), 84 ($FeCO^+$, 100), 56 (Fe^+, 93). IR, KBr, *v* (cm^{-1}): 3049 w, 2911 w, 2845 w, 2062 s, 2027 s, 1996 s, 1980 vs, 1967 s, 1958 s, 1621 w, 871 w, 856 w, 824 w, 749 m, 627 m, 588 m, 562 m, 548 m, 475 m. ^{1}H NMR, 400 MHz, CD_2Cl_2, 293 K, δ (ppm): 4.87 (s, 2H, CH_2), 7.47–7.59 (m, 3H, CH), 7.60–7.68 (m, 1H, CH), 7.80–7.98 (m, 6H, CH), 8.00–8.07 (m, 2H, CH), 8.28 (s, 1H, CH), 8.78 (s, 1H, CH). ^{13}C NMR, 100.6 MHz, CD_2Cl_2, 293 K, δ (ppm): 70.43, 121.58, 123.41, 127.02, 127.14, 127.20, 127.51, 127.98, 128.20, 128.26, 128.75, 129.02, 129.10, 129.73, 132.22, 133.64, 134.84, 136.63, 143.98, 148,96, 160.78, 210.69.

3.5. MS and spectroscopical data for 6

Anal. Calc. for $C_{28}H_{16}N_2O_6Fe_2$: C, 57.18; H, 2.74; N, 4.76. Found: C, 56.52; H, 2.97; N, 4.41%. FAB MS *m*/*z* (%): 589 ($M + H^+$, 8), 560 ($M + H^+$–CO, 5), 532 ($M + H^+$–2CO, 7), 504 ($M + H^+$–3CO, 26), 476 ($M + H^+$–4CO, 20), 448 ($M + H^+$–5CO, 6), 420 ($M + H^+$–6CO, 20). IR, KBr, *v* (cm^{-1}): 3047 w, 2957 w, 2922 w, 2892 w, 2837 w, 2064 s, 2028 s, 1990 s, 1972 s,

Table 1
Crystal and intensity data for **6**, **7**, **11**, **12** and **13**

	6	**7**	**11**	**12**	**13**
Formula	$C_{28}H_{16}N_2O_6Fe_2$	$C_{17}H_9NO_6Fe_2$	$C_{16}H_9NO_9Fe_3$	$C_{20}H_{10}N_2O_6Cl_2Fe_2$	$C_{16}H_6NO_9ClFe_3$
Molecular weight (g mol^{-1})	588.13	434.95	526.79	556.90	559.22
Radiation	Mo Kα	Mo Kα	Mo Kα	Mo Kα	Mo Kα
Monochromator	graphite	graphite	graphite	graphite	graphite
T (K)	183	183	183	183	183
Crystal color	red	orange	red	red	red
Crystal size	$0.5 \times 0.2 \times 0.02$	$0.3 \times 0.1 \times 0.02$	$0.5 \times 0.3 \times 0.03$	$0.4 \times 0.1 \times 0.05$	$0.2 \times 0.05 \times 0.05$
a (Å)	12.3642(3)	14.1315(4)	7.2734(9)	7.6944(4)	7.125(1)
b (Å)	13.2762(5)	7.2308(2)	9.363(1)	9.1139(5)	11.834(2)
c (Å)	14.9414(6)	16.4641(5)	14.461(2)	15.8209(9)	11.845(2)
α (°)	90	90	95.833(8)	101.653(3)	89.276(9)
β (°)	97.39(2)	98.368(2)	100.879(9)	90.968(3)	83.87(1)
γ (°)	90	90	108.403(6)	96.199(4)	78.83(1)
V (Å^3)	2432.3(2)	1664.42(8)	903.8(2)	1079.4(1)	974.1(3)
Z	4	4	2	2	2
$F(000)$	1192	872	524	556	552
ρ_{calc} (g cm^{-3})	1.606	1.736	1.936	1.713	1.906
Crystal system	monoclinic	monoclinic	triclinic	triclinic	triclinic
Space group	$P2_1/n$	$P2_1/n$	$P\bar{1}$	$P\bar{1}$	$P\bar{1}$
Absorption coefficient (mm^{-1})	1.241	1.777	2.428	1.632	2.391
θ limit (°)	$2.02 < \theta < 27.46$	$1.78 < \theta < 27.45$	$2.33 < \theta < 27.57$	$2.30 < \theta < 27.43$	$2.47 < \theta < 27.46$
Scan mode	ω-scan, ϕ-scan	ω-scan, ϕ-scan	ω-scan, ϕ-scan	ω-scan, ϕ-scan	ω-scan, ϕ-scan
Reflections measured	9574	6953	6253	7715	5852
Independent reflections	5560	3808	4078	4880	4133
R_{int}	0.0327	0.0154	0.0551	0.0228	0.0409
Reflections observed ($F_o^2 > 2\sigma(F_o^2)$)	4207	3263	2343	3841	2711
Number of parameters	407	271	274	299	295
Goodness-of-fit	0.996	1.054	0.988	1.043	1.036
R_1	0.0348	0.0275	0.0568	0.0431	0.0578
wR_2	0.0731	0.0633	0.1069	0.0954	0.1131
Final diffraction map electron density peak (e Å^{-3})	0.320	0.264	0.512	0.742	0.579

1947 s, 808 m, 797 m, 772 m, 617 m, 590 m, 573 m, 556 m, 489 w. ^{1}H NMR, 200 MHz, CD_2Cl_2, 293 K, δ (ppm): 4.87 (s, 2H, CH_2), 7.42 (d, 1H, $J_{HH} = 8$ Hz, CH), 7.51–7.70 (m, 5H, CH), 7.81–7.89 (m, 1H, CH), 7.92–8.02 (m, 4H, CH), 8.03–8.12 (m, 1H, CH), 8.53 (s, 1H, CH), 8.73–8.79 (m, 1H, CH). ^{13}C NMR, 50.3 MHz, CD_2Cl_2, 293 K, δ (ppm): 70.54, 108.02, 124.65, 124.99, 125.83, 126.28, 126.73, 127.78, 127.99, 128.11, 128.91, 129.22 (2C), 129.63, 131.28, 131.86, 133.82, 134.39, 135.08, 143.32, 151,01, 153.85, 210.79.

3.6. MS and spectroscopical data for 7

$C_{17}H_9NO_6Fe_2$, FAB MS m/z (%): 379 (M^+, 72), 351 (M^+–CO, 12), 323 (M^+–2CO, 11), 295 (M^+–3CO, 10). IR, KBr, ν (cm^{-1}): 3379 m, 3054 w, 3029 w, 3013 w, 2964 w, 2924 w, 2845 m, 2065 s, 2040 s, 2018 m, 1995 s, 1976 s, 1961 s, 1947 s, 809 m, 777 m, 754 m, 748 w, 675 w, 628 m, 595 m, 587 m, 569 m, 546 m, 498 m, 485 w, 449 w, 426 w. ^{1}H NMR, 400 MHz, CD_2Cl_2, 293 K, δ (ppm): 2.02 (s, br, 1H, NH), 4.49 (s, 2H, CH_2), 7.33 (d, 1H, $J_{HH} = 8.8$ Hz, CH), 7.56–7.60 (m, 2H, CH), 7.76–7.80 (m, 1H, CH), 7.90–7.95 (m, 1H, CH), 7.89 (d, 1H, $J_{HH} = 8.8$ Hz, CH). ^{13}C NMR, 100.6 MHz, CD_2Cl_2, 293 K, δ (ppm): 65.44, 113.01, 125.43, 125.96, 127.79, 127.91, 129.28, 133.79, 134.20, 143.51, 153.03, 211.00.

3.7. MS and spectroscopical data for 9

Anal. Calc. for $C_{22}H_{16}N_2O_8Fe_2$: C, 48.22; H, 2.94; N, 5.11. Found: C, 48.02; H, 2.91; N, 5.04%. DEI MS m/z (%): 548 (M^+, 4), 520 (M^+–CO, 8), 492 (M^+–2CO, 6), 464 (M^+–3CO, 23), 436 (M^+–4CO, 14), 408 (M^+–5CO, 51), 380 (M^+–6CO, 100). IR, KBr, ν (cm^{-1}): 2940 w, 2838 w, 2066 s, 2024 vs, 1994 vs, 1970 s, 1926 m, 1903 w, 1599 m, 1592 m, 1514 m, 1468 m, 1437 w, 1335 w, 1302 w, 1262 m, 1229 m, 1168 w, 1029 w, 830 w, 790 w, 627 m, 610 w, 570 m, 553 w, 375 m. ^{1}H NMR, 200 MHz, $CDCl_3$, 293 K, δ (ppm): 3.78 (s, 3H, OCH_3), 3.82 (s, 3H, OCH_3), 4.26 (s, 2H, CH_2), 6.87–6.98 (m, 3H, CH), 7.31 (s, 1H, CH), 7.56–7.61 (m, 3H, CH), 7.68 (s, 1H, CH). ^{13}C NMR, 50.3 MHz, $CDCl_3$, 293 K, δ (ppm): 55.24, 55.40, 71.55, 110.36, 114.35 (2C), 122.64, 125.79, 126.34, 129.48 (2C), 131.33, 149.49, 152,27, 156.77, 161.75, 210.62.

3.8. MS and spectroscopical data for **10**

$C_{24}H_{16}N_2O_{10}Fe_3$ DEI MS m/z (%): 660 (M^+, 15), 604 (M^+–2CO, 37), 576 (M^+–3CO, 4), 548 (M^+–4CO, 7), 520 (M^+–5CO, 14), 492 (M^+–6CO, 19), 464 (M^+–7CO, 30), 436 (M^+–8CO, 25), 408 (M^+–2CO–$Fe(CO)_5$, 29), 380 (M^+–$Fe_2(CO)_6$, 67), 149 ($C_8H_9N_2O^+$, 84), 133 ($C_8H_7NO^+$, 66), 28 (CO, N_2, 100). IR, KBr, ν (cm^{-1}): 2054 s, 2012 vs, 1987 sh, 1962 s, 1607 w, 1509 m, 1252 s, 1168 m, 1017 m, 831 w, 563 m, 375 w. ^{1}H NMR, 400 MHz, CD_2Cl_2, 293 K, δ (ppm): 2.61, 2.64, 3.93, 3.96 (AB, 2H, CH_2), 3.76 (s, 3H, OCH_3), 3.81 (s, 3H, OCH_3), 4.22 (d, 1H, $^4J_{HH} = 2.2$ Hz, CH), 5.12 (d, 1H, $^3J_{HH} = 6.5$ Hz, CH), 6.54 (d of d, 1H, $^3J_{HH} = 6.5$ Hz, $^4J_{HH} = 2.2$ Hz, CH), 6.89 (d, 2H, $^3J_{HH} = 8.8$ Hz, CH), 7.55 (d, 2H, $^3J_{HH} = 8.8$ Hz, CH), 7.56 (s, 1H, CH). ^{13}C NMR, 100.6 MHz, CD_2Cl_2, 293 K, δ (ppm): 55.73, 56.53, 68.88, 74.80, 83.32, 87.39, 105.53, 114.59 (2C), 117.01, 127.01, 129.27 (2C), 141.91, 147.12, 161.81, 211.16, 213.66.

3.9. MS and spectroscopical data for **11**

$C_{16}H_9NO_9Fe_3$ DEI MS m/z (%): 527 (M^+, 7), 499 (M^+–CO, 15), 471 (M^+–2CO, 6), 443 (M^+–3CO, 11), 415 (M^+–4CO, 77), 387 (M^+–5CO, 43), 359 (M^+–6CO, 61), 331 (M^+–7CO, 87), 303 (M^+–8CO, 58), 301 ($C_8H_7NOFe(CO)_4^+$, 100), 245 ($H_3COPhCHN[Fe(CO)_2]^+$, 61), 189 ($H_3COPhCHNFe^+$, 34), 134 ($H_3COPhCHN^+$, 18), 133 ($H_3COPhCN^+$, 13), 112 $(Fe(CO)_2)^+$, 84 ($FeCO^+$, 9), 56 (Fe^+, 24), 28 (CO, N_2, 14). IR, KBr, ν (cm^{-1}): 3307 w, 2965 w, 2927 w, 2851 w, 2089 s, 2065 s, 2050 s, 2029 sh, 2005 vs, 1979 s, 1950 s,1941 s, 1931 s, 1603 m, 1510 m, 1465 w, 1335 w, 1301 w, 1263 m, 1107 m, 1032 m, 889 m, 828 w, 801 w, 578 s.

3.10. MS and spectroscopical data for **12**

Anal. Calc. for $C_{20}H_{10}N_2O_6Cl_2Fe_2$: C, 43.31; H, 1.81; N, 5.03. Found: C, 43.46; H, 1.99; N, 4.60%. DEI m/z (%): 556 (M^+, 7), 528 (M^+–CO, 8), 500 (M^+–2CO, 20), 472 (M^+–3CO, 27), 444 (M^+–4CO, 13), 416 (M^+–5CO, 27), 388 (M^+–6CO, 100). IR, KBr, ν (cm^{-1}): 2894 w, 2831 w, 2066 s, 2034 vs, 1994 vs, 1985 vs, 1972 s, 1963 s, 1596 w, 1576 m, 1560 m, 1469 w, 1429 m, 1360 m, 1264 m, 1232 m, 1076 m, 998 m, 935 w, 871 m, 813 m, 775 m, 748 m, 626 s, 599 m, 573 s, 557 m, 481 m. ^{1}H NMR, 400 MHz, $CDCl_3$, 293 K, δ (ppm): 4.34 (s, 2H, CH_2), 7.09 (d of d, 0.3H, $^3J_{HH} = 8.6$ Hz, $^4J_{HH} = 2$ Hz, CH), 7.22–7.34 (m, 2.4H, CH), 7.37–7.39 (m, 1H, CH), 7.49–7.54 (m, 2H, CH), 7.62–7.63 (m, 1H, CH), 7.69 (s, 1H, CH), 7.99 (d, 0.3H, $^3J_{HH} = 8.6$ Hz, CH). ^{13}C NMR, 100.6 MHz, $CDCl_3$, 293 K, δ (ppm): 70.98, 71.92, 124.72, 125.89, 125.96, 126.81, 126.97, 127.02 (2C), 127.12, 127.51, 127.58, 130.18 (2C), 130.67, 130.75, 131.09, 134.76, 134.90, 135.01(2C), 137.26, 140.95, 147.21, 148.24, 148.56, 152.52, 156.53, 209.68, 209.77.

3.11. MS and spectroscopical data for **13**

$C_{16}H_5NO_9ClFe_3$, DEI m/z (%): 559 (M^+, 18), 531 (M^+–CO, 23), 503 (M^+–2CO, 11), 475 (M^+–3CO, 25), 447 (M^+–4CO, 43), 419 (M^+–5CO, 100), 391 (M^+–6CO, 32), 363 (M^+–7CO, 73), 335 (M^+–8CO, 100), 307 (M^+–9CO, 32). IR, KBr, ν (cm^{-1}): 2090 s, 2060 s, 2028 sh, 2013 vs, 2001 vs, 1989 sh, 1983 vs, 1972 sh, 1951 s, 1567 m, 1437 w, 1264 w, 927 m, 792 m, 682 m, 670 m, 622 m, 613 s, 579 m, 556 s.

3.12. Catalytic ethylene insertion reactions

A 50 ml autoclave charged with 1 mmol **2** (308 mg), $Ru_3(CO)_{12}$ (0.03 mmol) and toluene (5 ml) was pressurized with ethene (20 bar) and heated at 140 °C overnight. After the reaction mixture was cooled to room temperature it was transferred to a Schlenk tube and all volatile material was removed under reduced pressure. The remaining oily residue was used to determine yields of the products **14** and **15** by NMR spectroscopy. Column chromatography on silica gel gave **15** as a colorless oil using mixtures of light petroleum (b.p. 40–60 °C) and CH_2Cl_2 (80/20) as the eluent. The spectroscopical data of **15** are identical with those reported in the literature [12]. Elution with pure CH_2Cl_2 yielded a bright yellow fraction from which **14** crystallizes as yellow needles upon slow removal of the solvent.

3.13. MS and spectroscopical data for **14**

Anal. Calc. for $C_{26}H_{24}N_2$: C, 85.67; H, 6.63; N, 7.68. Found: C, 85.50; H, 6.27; N, 7.53%. DEI m/z (%): 364 (M^+, 42), 335 (M^+–C_2H_5, 24), 195 ($C_{14}H_{13}N^+$, 20), 184 ($C_{13}H_{14}N^+$, 43), 183 ($C_{13}H_{13}N^+$, 36), 182 ($C_{13}H_{12}N^+$, 96), 181 ($C_{13}H_{11}N^+$, 100), 167 ($C_{13}H_{11}^+$, 95), 153 ($C_{11}H_7N^+$, 41), 139 ($C_{11}H_7^+$, 23), 127 ($C_{10}H_7^+$, 18). IR, KBr, ν (cm^{-1}): 2969 s, 2928 s, 1594 m, 1509 m, 1453 m, 1377 m, 1216 s, 1058 s, 822 vs, 801 vs, 748 s, 454 m. ^{1}H NMR, 200 MHz, $CDCl_3$, 293 K, δ (ppm): 1.33 (t, 6H, $^3J_{HH} = 7.5$ Hz), 3.04 (q, 4H, $^3J_{HH} = 7.5$ Hz), 7.41 (d, 2H,$^3J_{HH} = 8.4$ Hz, CH), 7.46–7.67 (m, 4H, CH), 7.84 (d, 2H,$^3J_{HH} = 7.9$ Hz, CH), 7.86 (d, 2H, $^3J_{HH} = 8.4$ Hz, CH), 8.82 (d, 2H, $^3J_{HH} = 7.9$ Hz, CH). ^{13}C NMR, 50.3 MHz, $CDCl_3$, 293 K, δ (ppm): 16.23, 27.33, 125.50, 125.73, 127.03, 127.18, 127.88, 128.31, 130.86, 131.68, 132.52, 143.84, 162.09.

4. Supplementary material

Additional material on the structure analyses is available from the Cambridge Crystallographic Data Centre by mentioning the deposition number

CCDC-215648 (**6**), CCDC-215649 (**7**), CCDC-215650 (**11**), CCDC-215651 (**12**) or CCDC-215652 (**13**).

Acknowledgements

The authors gratefully acknowledge financial support by the Deutsche Forschungsgemeinschaft (Collaborative Research Center "Metal Mediated Reactions Modeled after Nature", SFB 436).

References

[1] (a) W. Imhof, J. Organomet. Chem. 533 (1997) 31;
(b) W. Imhof, Inorg. Chim. Acta 282 (1998) 111;
(c) W. Imhof, A. Göbel, D. Ohlmann, J. Flemming, H. Fritzsche, J. Organomet. Chem. 584 (1999) 33;
(d) W. Imhof, Organometallics 18 (1999) 4845;
(e) W. Imhof, A. Göbel, J. Organomet. Chem. 610 (2000) 102;
(f) A. Göbel, G. Leibeling, M. Rudolph, W. Imhof, Organometallics 22 (2003) 759.

[2] (a) D. Berger, W. Imhof, J. Chem. Soc., Chem. Commun. (1999) 1457;
(b) D. Berger, W. Imhof, Tetrahedron 56 (2000) 2015;
(c) W. Imhof, D. Berger, M. Kötteritzsch, M. Rost, B. Schönecker, Adv. Synth. Catal. 343 (2001) 795.

[3] (a) M. Rep, J.-W.F. Kaagman, C.J. Elsevier, P. Sedmera, J. Hiller, U. Thewalt, M. Horacek, K. Mach, J. Organomet. Chem. 597 (2000) 146;
(b) A. Ohff, T. Zippel, P. Arndt, A. Spannenberg, R. Kempe, U. Rosenthal, Organometallics 17 (1998) 1649;
(c) T. Zippel, P. Arndt, A. Ohff, A. Spannenbeg, R. Kempe, U. Rosenthal, Organometallics 17 (1998) 4429;
(d) J.L. Kiplinger, D.E. Morris, B.L. Scott, C.J. Burns, Organometallics 21 (2002) 3073.

[4] R. Cohen, B. Rybtchinski, M. Gandelmann, L.J.W. Shimon, J.M.L. Martin, D. Milstein, Angew. Chem. 115 (2003) 1993.

[5] (a) M.M. Bagga, P.L. Pauson, F.J. Preston, R.I. Reed, J. Chem. Soc., Chem. Commun. (1965) 543;
(b) M. Kilner, C.J. Midcaft, J. Chem. Soc., Dalton Trans. (1974) 1620;
(c) G. Gervasio, P.L. Stanghellini, R. Rosetti, Acta Crystallogr., Sect. B 37 (1981) 1198;
(d) D. Bright, O.S. Mills, J. Chem. Soc., Chem. Commun. (1967) 245;
(e) A. Zimniak, J. Zachara, J. Organomet. Chem. 533 (1997) 45.

[6] (a) M.M. Bagga, W.T. Flannigan, G.R. Knox, P.L. Pauson, F.J. Preston, R.I. Reed, J. Chem. Soc. C (1968) 36;
(b) A. Zimniak, Pol. J. Chem. 66 (1992) 1051;
(c) N.S. Nametkin, V.D. Tyurin, V.V. Trusov, A.S. Batsanov, Y.T. Struchkow, J. Organomet. Chem. 219 (1981) C36;
(d) J. Zachara, A. Zimniak, Acta Crystallogr., Sect. C 54 (1998) 353.

[7] (a) N.S. Nametkin, V.D. Tyurin, A.I. Nekhaev, Y.P. Sobolev, M.G. Kondrat'aeva, A.S. Batsanov, Y.T. Struchkow, J. Organomet. Chem. 243 (1983) 323;
(b) N.S. Nametkin, V.D. Tyurin, V.V. Trusov, A.M. Krapivin, J. Organomet. Chem. 254 (1983) 654.

[8] A. Zimniak, J. Organomet. Chem. 645 (2002) 274.

[9] S.U. Son, K.H. Park, I.G. Jung, Y.K. Chung, Organometallics 21 (2002) 5366.

[10] (a) M.A. Andrews, H.D. Kaesz, J. Am. Chem. Soc. 101 (1979) 7238;
(b) M.A. Andrews, G. Van Buskirk, C.B. Knobler, H.D. Kaesz, J. Am. Chem. Soc. 101 (1979) 7245;
(c) M.A. Andrews, H.D. Kaesz, J. Am. Chem. Soc. 101 (1979) 7255;
(d) M.A. Andrews, C.B. Knobler, H.D. Kaesz, J. Am. Chem. Soc. 101 (1979) 7260.

[11] (a) F. Kakiuchi, M. Yamauchi, N. Chatani, S. Murai, Chem. Lett. (1996) 111;
(b) D. Berger, A. Göbel, W. Imhof, J. Mol. Catal. A 165 (2001) 37.

[12] R.R. Fraser, S. Savard, Can. J. Chem. 64 (1986) 621.

[13] (a) G. Sheldrick, SHELXS-86, Universität Göttingen, 1986;
(b) G. Sheldrick, SHELXL-93, Universität Göttingen, 1993.

[14] L. Zsolnai, G. Huttner, XPMA, Universität Heidelberg, 1996.

[15] Siemens Analytical X-ray Inst. Inc., XP – Interactive Molecular Graphics, Vers. 4.2, 1990.